Advanced Laboratory Experiments
Universität Siegen
Prof. Dr. I. Fleck

Part-I: Beta Spectroscopy

Abstract

The experiment on beta spectroscopy introduces the student into the field of special relativity and weak interactions of radioactive decays. With the help of a simple silicon semiconductor spectrometer, the continuous spectra of some beta-ray emitters should be measured and interpreted.

Key words: semiconductor, beta decay, internal conversion, auger electron, Photoeffect, Compton scattering

Literature

T. Mayer-Kuckuk *Kernphysik*, Teubner 2002

W.S.C. Williams *Nuclear and Particle Physics*, Clarendon Press Oxford 1991

C. Grupen *Particle Detectors*, Cambridge University Press 1996, 2008

Glenn F. Knoll *Radiation Detection and Measurements*, John Wiley & Sons, Inc. 2000

Contents

1 Experimental Setup

The experimental setup is shown in Fig. 1. It consists of a silicon-lithium drifted PIN detector to record the electron spectra. The detector is supplied with a positive high voltage from a DSG (TYP 103A) high voltage supply. It is important that the voltage should not exceed 600 V, corresponding to a setting of 0.60. The bias voltage for the detector should be connected to the preamplifier from EG&G, model 142 AG.

The signals are fed into this preamplifier and from there into the main amplifier, which is an Ortec 570 model. It is important to set the coarse gain to 200, the fine gain to 6.50 or somewhere around that value, shaping time 0.5 μs, positive polarity and automatic base line restoration. The signals are then unipolar. They should be viewed on a scope and fed into the multi-channel analyser which can be read out by a computer or some other appropriate means.

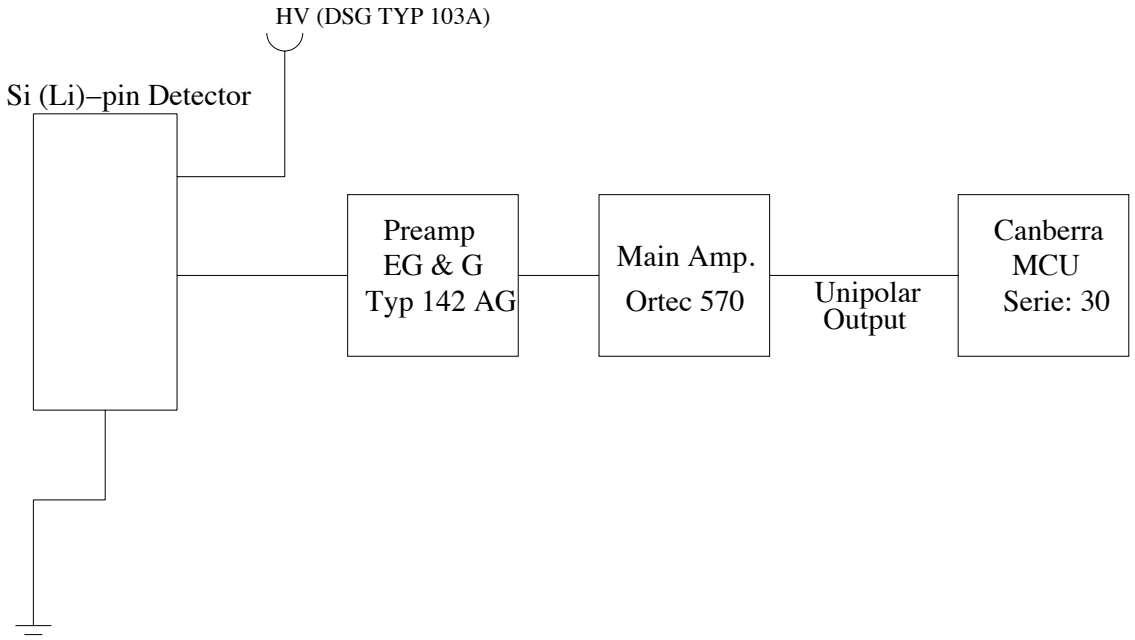

Figure 1: Experimental Setup

2 Measurement Principle

A lithium-drifted silicon semiconductor counter measures the kinetic energy of electrons. The electrons lose their energy in the intrinsic conducting layer of the PIN detector by producing electron-hole pairs. The number of produced charge carriers is proportional to deposited energy. On average 3.65 eV is required to produce an electron-hole pair in silicon. The charge carriers which are produced by the incident electrons are drained with the help of an external electric field, leading to a charge signal. This signal is amplified by a charge sensitive preamplifier and fed to the voltage sensitive main amplifier. This main amplifier provides voltage signals in a suitable dynamical range which can be processed by a multi-channel analyzer. The measured channel number on the multi-channel analyzer is proportional to the deposited energy in the detector. To convert the channel numbers to energies, a calibration of the complete detector system is required. The calibration is performed with an electron capture emitter (Bi 207). This

radioisotope emits monoenergetic electrons from the K-shell at 482 keV, 972 keV and 1682 keV which cover a large range of electron energies to be measured.

3 Basics of Beta Decay

3.1 Relativistic Energy Momentum Relation

In the framework of Einstein's theory of relativity, energy and mass are equivalent:

$$E = mc^2 \quad .$$

The relativistic mass is a function of the velocity:

$$m = \frac{m_0}{\sqrt{1-\beta^2}} = \gamma m_0 \qquad , \quad \beta = \frac{v}{c} \quad .$$

Using these two relations, we find the following formulae:

$$\begin{aligned} m^2(1-\beta^2) &= m_0^2 \\ \underbrace{m^2c^4}_{E^2} - \underbrace{m^2v^2}_{p^2}c^2 &= m_0^2c^4 \\ E &= \sqrt{m_0^2c^4 + p^2c^2} = c\sqrt{p^2 + m_0^2c^2} \end{aligned}$$

using the kinetic energy $E_{\text{kin}} = E - m_0c^2$ we obtain:

$$E_{\text{kin}} = c\sqrt{p^2 + m_0^2c^2} - m_0c^2$$

or correspondingly:

$$cp = \sqrt{E_{\text{kin}}(E_{\text{kin}} + 2m_0c^2)} \quad .$$

3.2 Beta Decay

There are three different kinds of beta decays:

1. β^- decay: $n \to p + e^- + \overline{\nu}_e$
2. β^+ decay: $p \to n + e^+ + \nu_e$
3. electron capture (EC): $p + e^- \to n + \nu_e$

β^- and β^+ decays are three-body processes. Hence, the energy spectra of electrons or positrons are continuous. Historically, when the continuous beta-ray spectra was first observed, the interpretation of it was a problem as it appeared that the energy conservation was violated. Introducing neutrinos to explain the continuous beta-ray spectra solved not only the problem of momentum and angular momentum conservation but additionally, the conservation of lepton number.

The transition energies can be calculated as follows:
Let $M(Z, A)$ be the atomic mass, then $M(Z, A) - Z \cdot m_e$ is the mass of the nucleus.

1. β^- decay: $M(Z,A) \rightarrow M(Z+1,A)+e^-+\overline{\nu}_e$ The energy difference for β^- decay is obtained by comparing the mass of the initial parent nucleus and the mass of the daughter nucleus:

$$\begin{aligned}\Delta E_1 &= [\quad \underbrace{\{M(Z,A)-Zm_e\}}_{\text{mass of the parent nucleus}} \quad -\{\underbrace{M(Z+1,A)-(Z+1)m_e}_{\text{mass of the daughter nucleus}} +m_e\}]c^2 \\ &= \{M(Z,A)-M(Z+1,A)\}c^2\end{aligned}$$

2. β^+ decay: $M(Z,A) \rightarrow M(Z-1,A)+e^+ +\nu_e$

$$\begin{aligned}\Delta E_2 &= [\{M(Z,A)-Zm_e\}-\{M(Z-1,A)-(Z-1)m_e+m_e\}]c^2 \\ &= \{M(Z,A)-M(Z-1,A)-2m_e\}c^2\end{aligned}$$

3. electron capture: $M(Z,A)+m_e \rightarrow M(Z-1,A)+\nu_e$

$$\begin{aligned}\Delta E_3 &= [\{M(Z,A)-Zm_e+m_e\}-\{M(Z-1,A)-(Z-1)m_e\}]c^2 \\ &= [M(Z,A)-M(Z-1,A)]c^2 \quad .\end{aligned}$$

Beta decay can only occur if the energy difference $\Delta E_i > 0$ $(i = 1,2,3)$. β^+ decay is in competition with electron capture as long as $\Delta E_3 > 2m_ec^2$, otherwise (for $0 < \Delta E_3 < 2m_ec^2$) only electron capture can occur.

Free neutrons are unstable because $m_n > m_p + m_e + m_{\overline{\nu}}$. For similar reasons free protons cannot decay. For nucleons in a nucleus the energy difference ΔE can take on positive as well as negative values.

The transition energy ΔE is shared essentially between the kinetic energies of electons and neutrinos. The kinetic energy of the recoil nucleus is usually very small and can be neglected. Since the daughter nucleus is generally reached in an excited state the following energy relations can be formulated:

$$\begin{aligned}E_{e^-}+E_{\overline{\nu}}+E_\gamma = E_{\beta^-_{\max}}+E_\gamma &= \Delta E(\beta^-) \\ E_{e^+}+E_\nu+E_\gamma = E_{\beta^+_{\max}}+E_\gamma &= \Delta E(\beta^+)-2m_ec^2\end{aligned}$$

If the parent nucleus decays directly into the ground state of the daughter nucleus no photons are emitted.

At low energies the energy spectra of electrons and positrons are distinctly different due to a Coulomb correction (Fermi correction) (see also Fig. 2).

3.3 Energy Spectra

Fermi's theory of beta decay provides the means to determine the momentum spectra of electrons

$$N(p_\beta)\mathrm{d}p_\beta = \frac{g^2|M|^2}{2\pi^3\hbar^7c^3}(E_\beta^{\max}-E_\beta)^2p_\beta^2\mathrm{d}p_\beta$$

where g is the coupling constant of weak interactions,
M – the nuclear matrix transition element,

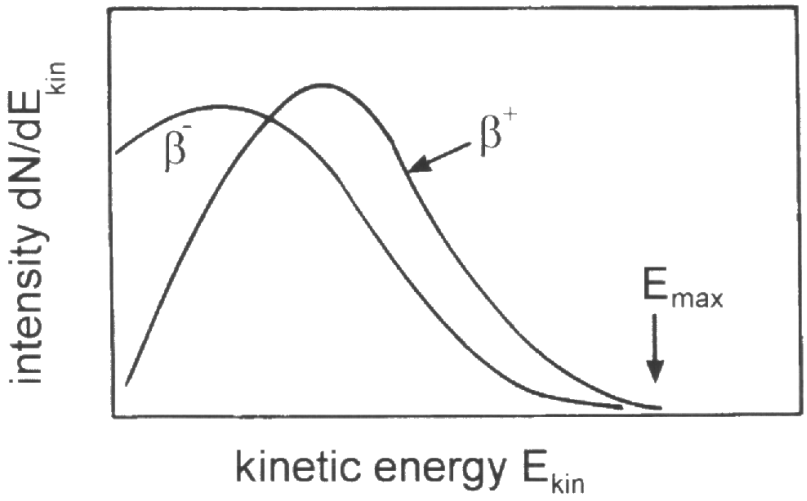

Figure 2: Continuous β^- and β^+ spectra

p_β, E_β – electron momentum and electron energy;
using $E_\beta = m_0c^2 + E_{\rm kin}$ and dividing by the rest energy m_0c^2 one obtains

$$\begin{aligned} w &= E_\beta/m_0c^2 = 1 + E_{\rm kin}/m_0c^2 \\ w_0 &= E_\beta^{\rm max}/m_0c^2 = 1 + E_{\rm kin}^{\rm max}/m_0c^2 \quad . \end{aligned}$$

Defining

$$\eta = \frac{p}{m_0c}$$

one gets

$$w^2 = \eta^2 + 1 \quad .$$

This leads to momentum spectrum of

$$N(\eta)\mathrm{d}\eta = \mathrm{const} \cdot (w_0 - w)^2 \cdot \eta^2 \cdot \mathrm{d}\eta$$

because of $w\mathrm{d}w = \eta\mathrm{d}\eta$ the energy spectrum of electrons is obtained as

$$\begin{aligned} N(w)\mathrm{d}w &= \mathrm{const}(w_0 - w)^2 \cdot \eta w \mathrm{d}w \\ &= \mathrm{const}(w_0 - w)^2 \cdot w\sqrt{w^2-1}\mathrm{d}w \quad . \end{aligned}$$

Finally we incorporate an extra factor, the Coulomb correction factor $F(Z, w)$ to account for the interaction of the electron which leaves the nucleus and the electrostatic field of the daughter nucleus

$$N(w)\mathrm{d}w = \mathrm{const}(w_0 - w)^2 \cdot w\sqrt{w^2-1} \cdot F(Z,w)\mathrm{d}w \quad .$$

$F(Z, w)$ is called the Fermi function:

$$F(Z,w) = \frac{2\pi a_Z}{1 - e^{-2\pi a_Z}} \qquad with \qquad a_Z = \frac{Z\alpha w}{\sqrt{w^2-1}} \quad ,$$

where $\alpha = \frac{1}{137}$ is the electromagnetic fine-structure constant and Z is the atomic number of the daughter nucleus. In case of β^+ decay $F(Z,w)$ is to be replaced with $F(-Z,w)$.

It is difficult to read the maximum electron energy (which is the transition energy) from the energy spectra plotted in this way. Therefore, to work out an exact value of the transition energy the energy spectrum is linearized in the following way:

$$w_0 - w = \{N(w)[\text{const} \cdot w\sqrt{w^2-1} \cdot F(Z,w)]^{-1}\}^{1/2} \quad .$$

The constant in this analysis has no meaning and can be approximated with 1. Thus, instead of $w_0 - w$ we calculate $f(w)$ which is

$$f(w) = \sqrt{\frac{N(w)}{w\sqrt{w^2-1} \cdot F(Z,w)}} \quad ,$$

where $N(w)$ is the number of β particles for $w = \frac{E}{m_e \cdot c^2}$. This is a linear representation of the beta energy spectrum (Kurie plot). The Kurie plot (also named Fermi plot or Fermi-Kurie plot), which is a representation of the function $f(w)$ versus w (Fig. 3), allows to read w_0 and the transition energie $E_{kin}^{max} = (w_0 - 1) \cdot m_e c^2$ easily and directly from the linear fit of the Kurie plot $f(w) = a \cdot w + b$, where $w_0 = -\frac{b}{a}$.

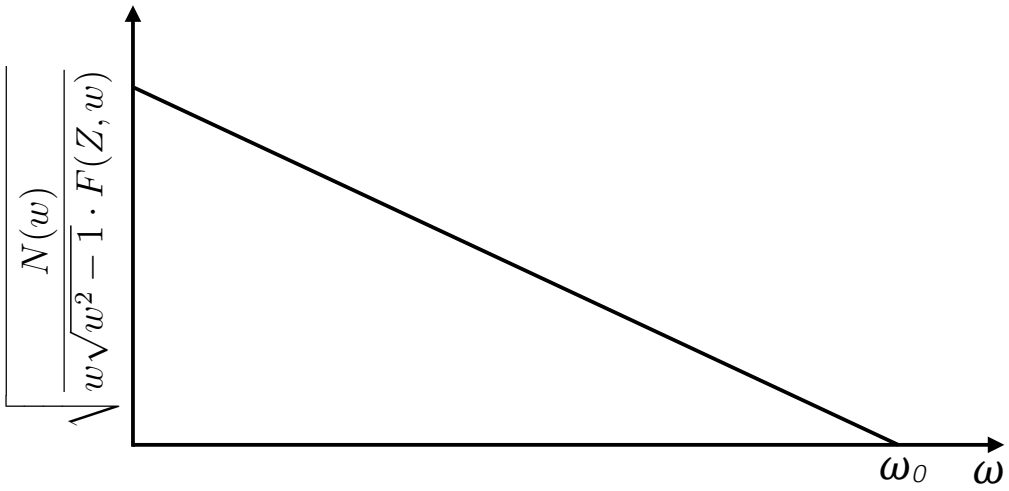

Figure 3: Femi-Kurie Plot of the β Spectrum

It has to be mentioned that the Kurie plots of electron energy spectra are only completely linear if the transitions are allowed (i.e. the nuclear matrix transition element is approximately constant).

3.4 Monoenergetic Electron Lines

Superimposed on the continuous beta spectra there are monoenergetic electron lines. These are at the low end of the energy spectrum Auger electrons or at the higher end conversion electrons. Auger electrons are produced if the excitation energy of the atomic shell is used to liberate electrons, so these Auger electrons have typically energies of several keV while conversion electrons are produced if the excitation energy of a nucleus is transferred in a direct fashion to electrons in the K-, L- or M-shell (see also Fig. 5).

3.5 Decay Schemes of Some Typical Electron Emitters

Bi 207 conversion electrons emitted from K and L shells:

$$E_\beta^1 = \begin{cases} 0.482\,\text{MeV} & \text{K-shell} \\ 0.554\,\text{MeV} & \text{L-shell} \end{cases}$$

$$E_\beta^2 = \begin{cases} 0.972\,\text{MeV} & \text{K-shell} \\ 1.044\,\text{MeV} & \text{L-shell} \end{cases}$$

$$E_\beta^3 = \begin{cases} 1.682\,\text{MeV} & \text{K-shell} \\ 1.754\,\text{MeV} & \text{L-shell} \end{cases}$$

$$E_\beta^4 = \begin{cases} 1.354\,\text{MeV} & \text{K-shell} \\ 1.426\,\text{MeV} & \text{L-shell} \end{cases}$$

4 How To Do the Experiment

4.1 Check-up of the Spectrometer

The semiconductor spectrometer is operated with positive high voltage of up to 600 V. **Never** switch on or off the full voltage in one go. Please consider also that the detector should not be exposed to daylight if the voltage is on.

Increase the high voltage on the detector slowly until the operating voltage is reached. This corresponds to a reading of the potentiometer of ~ 0.60. Measure the signal shape after the preamplifier and after the main amplifier and make a sketch of these signal forms and please also note all the chosen parameters (main amplifier, multi-channel analyser and radioactive source).

4.2 Background Measurement

Measure the background (without radioactive source) at reasonable statistics (measurement time at least one day, maybe even longer than that). Interpret the shape of the background spectrum and its possible structures. What are the reasons for bumps and peaks in the energy loss or in the energy? Subtract the background from your further measurements.

4.3 Calibration

The calibration is done by recording the energy spectrum of conversion electrons from the electron capture emitter Bi 207. The electrons always make two peaks close to each other, as electrons can be emitted from K- and L- shells. Use only the first two pairs of peaks for the calibration. Make a simultaneous fit to the two peaks of one pair and the underlying background events. Find the channel numbers which correspond to the maximum of these peaks. Make a plot where the channel number is plotted against the energy and determine the calibration function.

4.4 Experimental Measurement of Some Beta Ray Emitters

Record the beta ray spectra of the radioisotopes Co 60, Cs 137 and also the beta ray spectrum of some unknown source. Analyze the beta ray spectra with the help of Kurie plots and determine the transition energies. In the case there are two β-decays for one radioisotope think carefully on how to determine the transition energies.

4.5 Compton Edges

Explain the process of Compton scattering and determine the photon energies of all visible Compton edges (e.g., in the Bi 207 spectrum).

4.6 Statistical and Systematic Uncertainties

Describe how the statistical error from the calibration affects your measurement. Determine for all experimental results statistical and systematical errors.

4.7 Conversion Energy

Determine the conversion energies in the Cs 137 spectrum.

4.8 Graphical Representation

Plot all data in a graphical way (on linear **and** semi-logarithmic scales). Please discuss all experimental results and provide graphs of energy spectra and Kurie plots for all measured sources.

4.9 Summary

Make a summary table with all measured results, their uncertainties, and the values from literature. Interpret your measurements.

5 Problems

a) Determine the energy resolution of the detector with the help of data from the calibration spectrum and compare the results with theoretical estimates.

b) Determine the relativistic mass increase $\Delta m/m$ for electrons of kinetic energy 1.18 MeV (transition energy of Cs 137).

c) The decay chain Sr 90 $\rightarrow$ Y 90 $\rightarrow$ Zr 90 consists of a parent nucleus with a half life of $T_{\mathrm{Sr}} = 28.5\,\mathrm{a}$ and a daughter nucleus with half life of $T_{\mathrm{Y}} = 64.1\,\mathrm{h}$. The following quantities are to be plotted in a semi-logarithmic plot for the first 100 h:

   1. The activity of the parent nucleus $N_{\mathrm{Sr}}(t)$, for an initial activity of $\dot{N}_{\mathrm{Sr}}(t = 0) = 1\,\mathrm{mCi} = 3.7 \cdot 10^7\,\mathrm{Bq}$.
   2. The activity $N_{\mathrm{Y}}(t)$ for the daughter product with $N_{\mathrm{Y}}(t = 0) = 0$.

d) What is the range of a 2 MeV electron in silicon?

6 Appendix A: Manual Information on the Detector and the Readout Electronics

a) **Detector:**
Si(Li) detector, 3 mm intrinsic layer, 1250 mm^2 sensitive area, manufacturer: KEVEX
Please **never** switch off the detector. If it is to be disconnected from the power supply the high voltage must be reduced slowly and later on if the detector is going to be switched on again the high tension must be increased rather slowly up to the working voltage.
The detector is sensitive to light (like a silicon solar cell). **Never** expose the detector to full daylight if it is under high voltage.

The energy resolution of the detector system at the time of production was

4.3 keV at 0pF load
7.3 keV at 50 pF load.

The maximum achieved energy resolution was

$\frac{\Delta E}{E} = 1.4\%$ for the 976 keV Bi 207-line

corresponding to 14 keV FWHM at 500 V bias voltage.

b) **Preamplifier:**
Preamplifier 142 IH Ortec/EG&G.

c) **Main amplifier:**
Model 570 Ortec/EG&G.

d) **High voltage power supply:**
DSG TYP 103A
This high voltage system can supply a maximum voltage of 5000 V. The polarity can be chosen. It **has to be positive** for the detector and should **never** exceed 600 V (which is 0.60 on the scale of the meter).
The potentiometer is linearly subdivided (5000 V $\hat{=}$ 5 turns on the potentiometer).

e) **Range and energy loss plots for electrons in silicon**:

7 Appendix B: Documentation Describing the Analysis Procedure Using the Computer

The experimental data are recorded in a multichannel analyzer model Canberra 30. The data are read out by the I/0-function into the memory of an Atari computer and can be stored on

disk. The processing of the data on disk can be done directly on the Atari or – after appropriate adaptions – on any PC.

The program running on the Atari (Canberra.PRG) is menu-operated and more or less self explaining. Data are read from MCA or disk. They can be labelled and/or modified.

For further operating details contact the instructor.

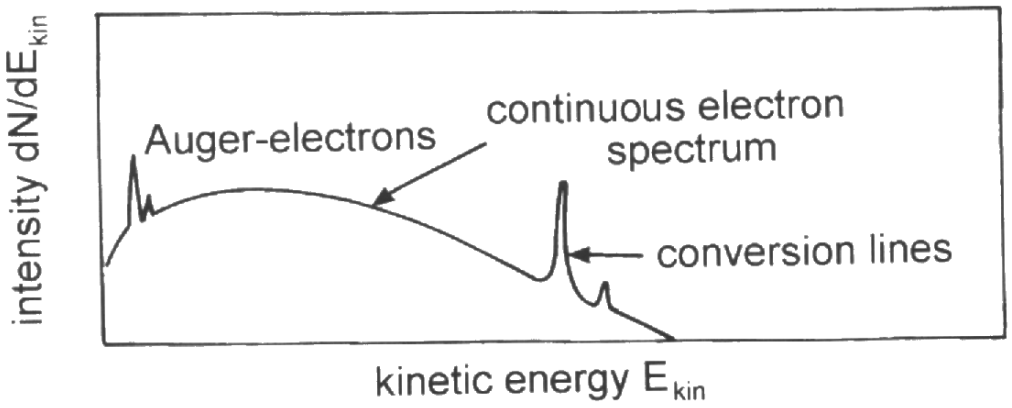

Figure 4: Continuous electron spectrum with characteristic Auger and conversion lines

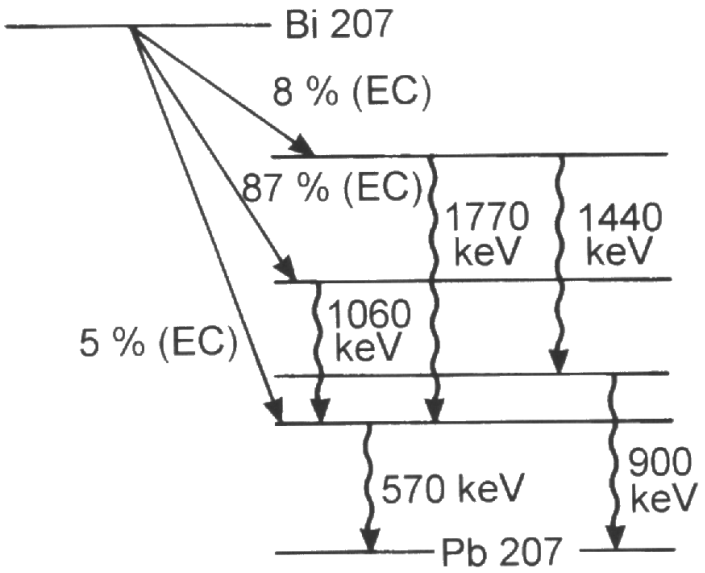

Figure 5: Calibration source Bi 207 (EC - electron capture)

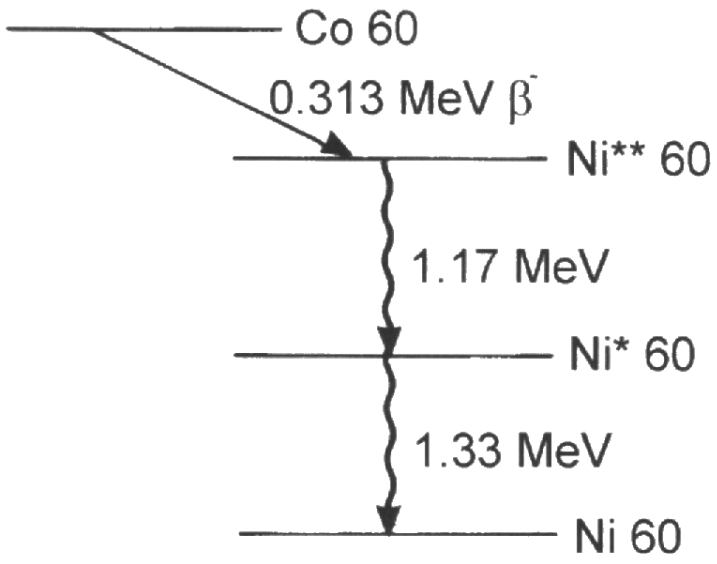

Figure 6: Co 60

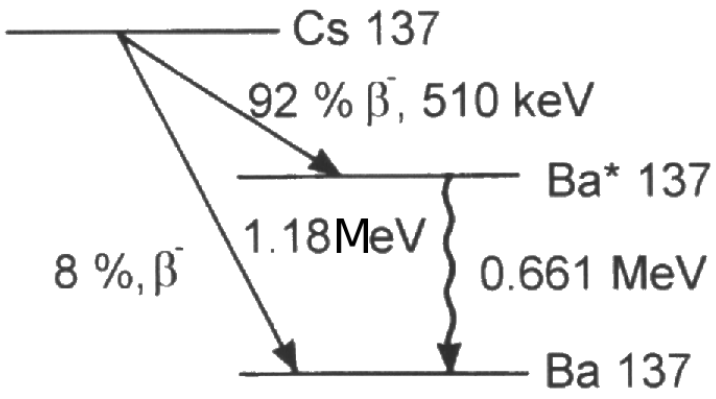

Figure 7: Cs 137

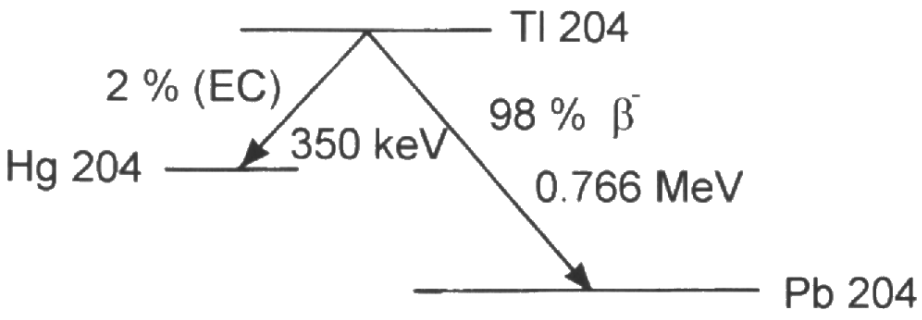

Figure 8: Tl 204

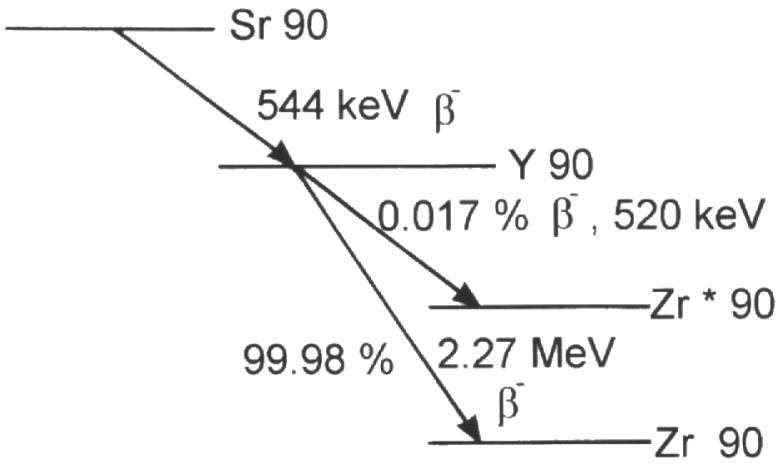

Figure 9: Sr 90 → Y 90 → Zr 90

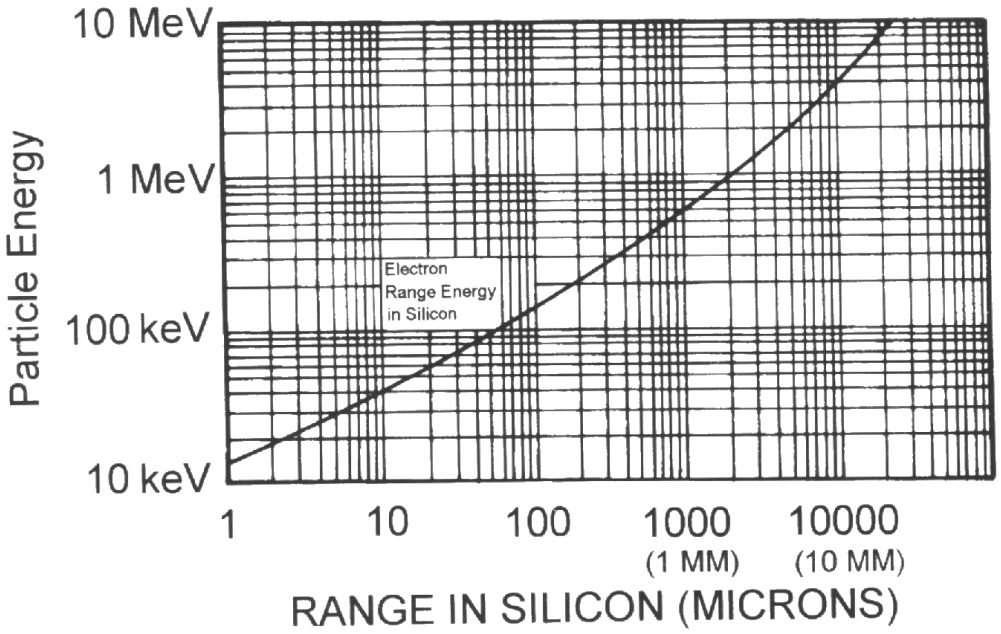

Figure 10: Energy-range relation for electrons in silicon

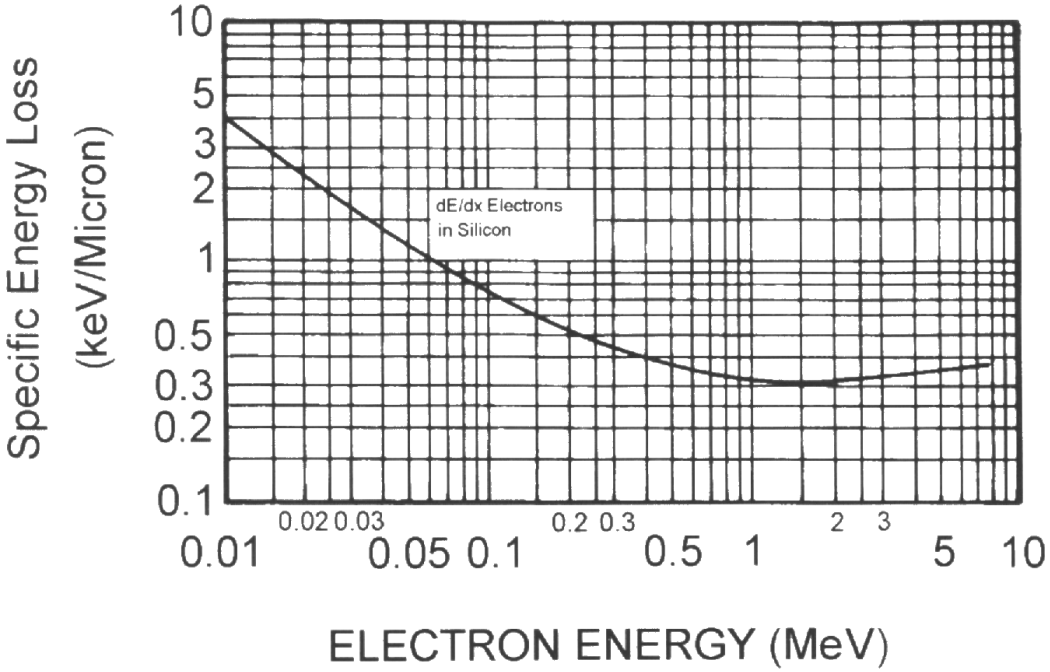

Figure 11: Energy-loss relation for electrons in silicon

Part-II: Characterisation of SiPM detector using an ultra-fast pulsed LED

Amartya Rej, Prof. Dr. Ivor Fleck

Department Physik
Universität Siegen, 57072 Siegen, Germany

1 Introduction

Silicon Photomultipliers (SiPM) are the new technology used in many important physics experiments as a photon counting device. They are very appealing for different reason: a) high detection efficiency (single photo-electron discrimination), b) compactness and robustness c) low operating voltage and power consumption, d) low cost, e) withstanding to magnetic field. These features make this technology fashionable in different application fields i.e. medical applications, homeland security, spectrometry or high energy physics.

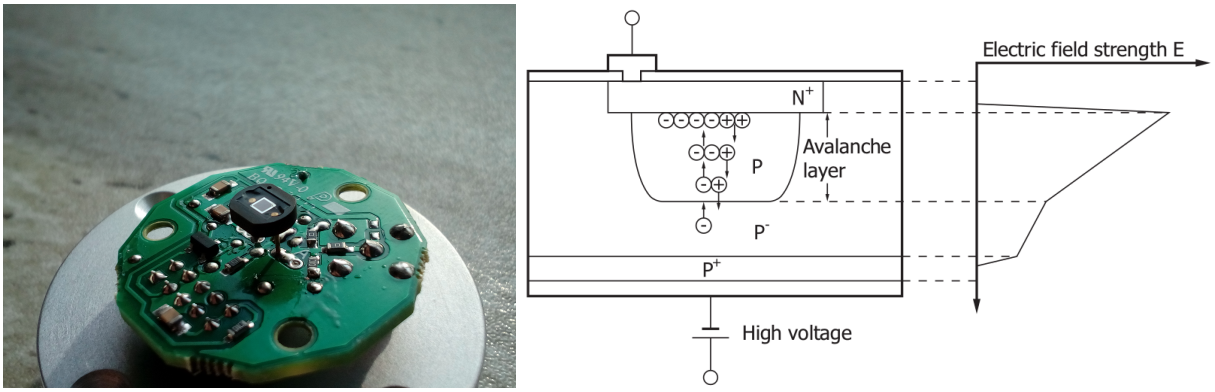

Figure 12: A Hamamatsu S13360-1350CS SiPM on a circuit board (left); the avalanche multiplication (right)

Silicon Photomultipliers (SiPM) consist of a high-density matrix (up to $10^4/\text{mm}^2$) of Avalanche Photo Diodes (APD) connected in parallel on a common Si substrate. When light enters an APD with a reverse voltage applied to the p-n junction, electron-hole pairs are generated in the depletion layer if the light energy is higher than the band gap energy. The electric field created across the p-n junction (figure 12) causes the electrons to drift toward the N^+ side and the holes to drift toward the P^+ side. The higher the electric field, the higher the drift speed of these carriers. However, when the electric field reaches a certain level, the carriers are more likely to collide with the crystal lattice so that the drift speed becomes saturated at a certain speed. If the electric field is increased even further, these carriers colliding with the crystal lattice generates new electron-hole pairs, which is called ionization. These electron-hole pairs then create additional electron-hole pairs, which generate a chain reaction of ionization. This phenomenon is known as avalanche multiplication.

Each APD is operated in a limited Geiger regime connected in series with a quenching resistor in order to achieve gain at level of 10^6. There are 667 APDs(pixels) having pixel pitch of 50 μm, packed in a area of 1.3mm x 1.3mm in the SiPM. As a consequence these detectors are sensitive to single photon detection even at room temperature. This features a dynamic range well above 100 photons and have a high Photon Detection Efficiency (PDE) up to 40%. The spectral dependence of the PDE is shown in figure 14. SiPMs measure the light intensity simply by the number of fired cells. However, this information is affected and biased by stochastic effects characteristic of the sensor and occurring within the time window: spurious avalanches due to thermally generated carriers (referred to as **dark counts**), delayed avalanches associated to the release of carriers trapped in metastable states (referred to as **afterpulses**) and an excess of fired cells due to photons produced in the primary avalanche, travelling in silicon and triggering neighboring cells (a phenomenon called **optical cross talk**).

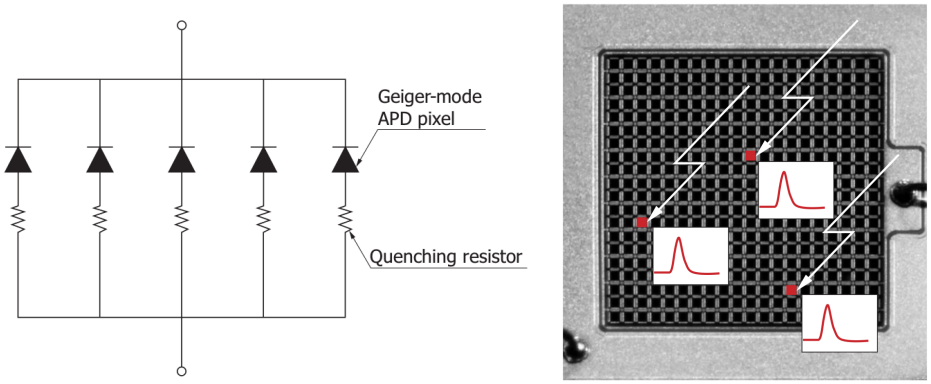

Figure 13: Equivalent circuit of a SiPM: each pixel provides information on whether or not it is fired

In this experiment, various experimental issues of an SiPM will be studied as well as operating points have to be determined when counting photons from a pulsed LED.

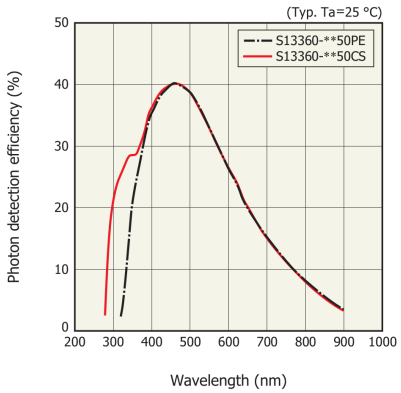

Figure 14: Spectral response of Photon Detection Efficiency of the SiPM

2 Basic Operation

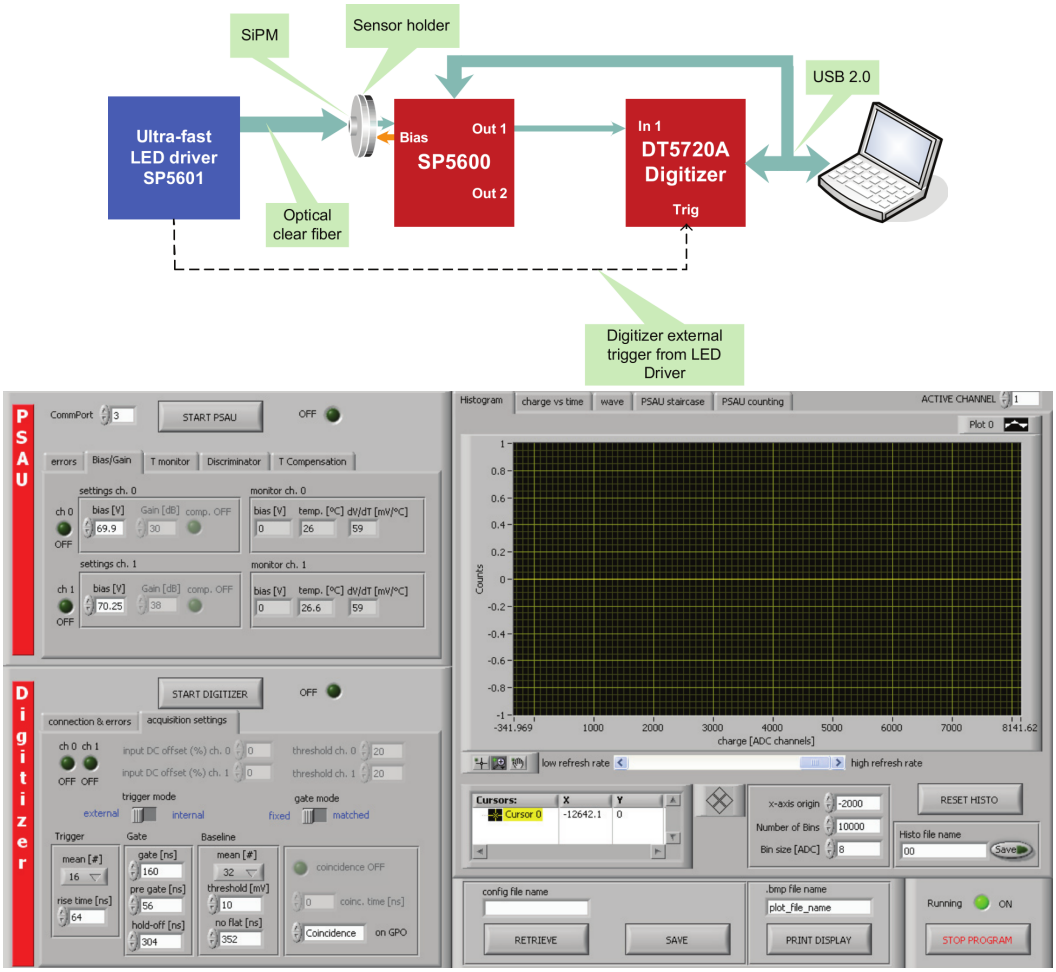

Figure 15: The block diagram of the experimental setup (top); The LabView GUI (bottom)

A Hamamatsu S13360-1350CS SiPM is used for the purpose of this experiment. The basic connections of the components of the experiments have to be made following figure 15 (top). The components include an ultra-fast LED pulse generator, giving the light pulse through an optical fiber to the SiPM attached by a sensor holder and plugged to a Power Supply Amplification Unit (PSAU), which gives the proper bias voltage, V_B and amplification, G_{PSAU}. The output is connected to a Desktop Digitizer and triggered either with the LED driver or internally triggered. The PSAU and the digitizer are operated by interfacing to a computer with a LabView graphical user interface (GUI) support as shown in figure 15 (bottom).

To start with, the PSAU can be set to a reverse bias voltage of 53V and a gain of 40 dB. The waveform coming from the electrons produced by the detected photon can look like as in figure 16. To capture the signal, a proper trigger should be set with the **gate** (trigger) window and the **baseline** (average noise, to be used as zero) parameters, computing the waveform integral (area below the baseline) to get the output charge corresponding to the detected photon. A gate of 192ns with pregate of 56ns and hold off of 504ns is suggested to be used with a baseline of mean 256, threshold 8mV and no-flat time of 512 ns.

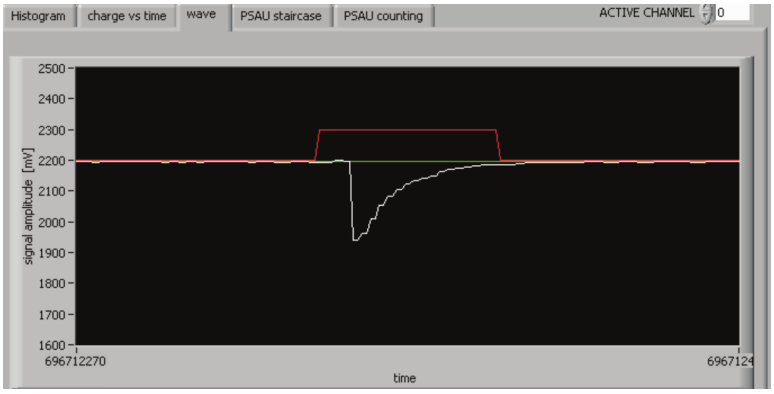

Figure 16: A sample picture of the waveform with the shown trigger gate and baseline

3 Features of SiPM and Measurements

With the above mentioned settings, the measured charge can be found quantized, corresponding to the number of photo-electrons fired in the SiPM cells. An example of the charge spectrum can be found in figure 17. The number of photo-electrons fired are called photon equivalent or p.e.

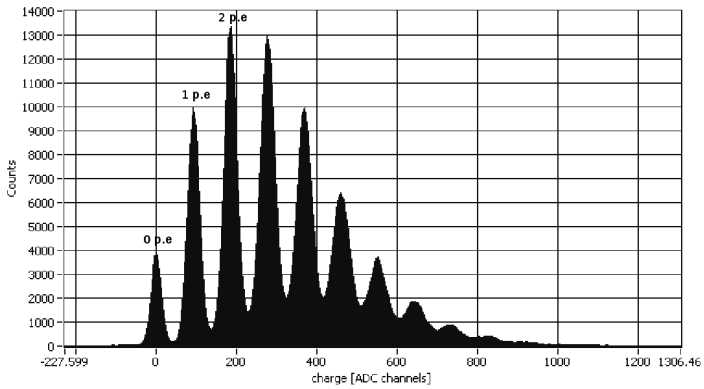

Figure 17: A charge spectrum with visible photo-electron peaks

3.1 Visualisation of cross talk and afterpulse phenomena

Optical cross talk: When light enters one SiPM pixel, there may be cases where a pulse of 2 p.e. or higher is observed. This is because secondary photons are generated in the avalanche multiplication process of the SiPM pixel and those photons are detected by other pixels. This phenomenon is called optical cross talk.

Afterpulse: During the avalanche multiplication process in SiPM pixels, the generated carriers may be trapped by lattice defects. When these carriers are released after a certain time, new avalanches are produced along with the photon-generated carriers and are then observed as afterpulses. The afterpulses are not distinguishable by shape from photon-generated pulses. Both the phenomena are shown in figure 18 as a running snapshot of the SiPM output waveform.

TASK: Try to take a snapshot showing the afterpulses if any. The cross talk phenomenon visualisation is possible (quantitatively) in the next sections only, considering that a running snapshot(as in the figure) is not possible in the used device.

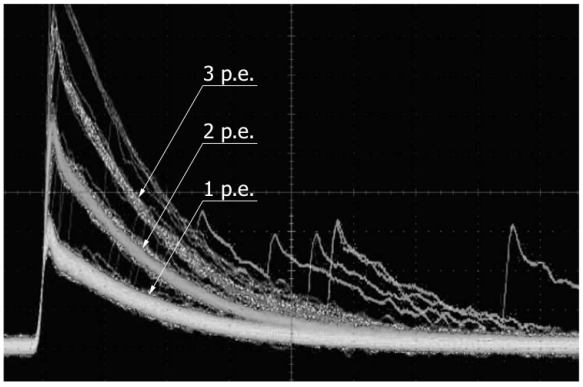

Figure 18: Optical cross talk and afterpulse phenomena

3.2 Dark count and cross talk measurement

In the SiPM pulses are produced not only by photon-generated carriers but also by thermally-generated carriers. The pulses produced by the latter are called the dark pulses. The dark pulses are observed along with the signal pulses and so cause detection errors. Thermally-generated carriers are also multiplied to 1 p.e. signal level. The **dark count** of the SiPM is defined as the number of pulses that are generated in a **dark state** (with no light) and exceed a threshold of 0.5 p.e. This is expressed as $N_{0.5}$ p.e. The number of dark pulses per second is termed as the **dark count rate (DCR)** [unit: cps (counts per second)]. The cross talk probability is calculated as:

$$P_{cross\text{-}talk} = \frac{N_{1.5}\text{ p.e}}{N_{0.5}\text{ p.e}} \tag{1}$$

The cross talk probability depends on the applied reverse bias voltage. For the measurement of the dark counts in the dark state the internal trigger of the digitizer should be used. A threshold of around 20 can be set for the internal trigger.

TASK: Calculate the cross talk probability in a dark state. Vary the applied reverse bias voltage with small steps and create a plot of cross talk probability, $P_{cross\text{-}talk}$ vs reverse voltage(V) as in figure 19.

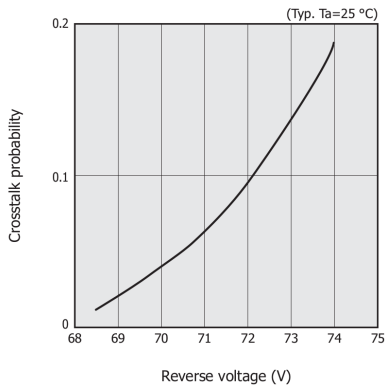

Figure 19: Cross talk probability vs bias voltage

3.3 Dark Count Rate (DCR) measurement for trigger threshold determination

The frequency of the dark counts is called the Dark Count Rate (DCR). For an actual measurement of any photon source, the DCR should be kept low. One technique to reduce it is to increase the trigger threshold voltage. To understand the optimum trigger threshold voltage, a staircase plot of the DCR vs threshold voltage can be drawn using the "PSAU Staircase" option in the LabView GUI, see figure 20. This works for internal trigger only and the set threshold beforehand does not affect the staircase plot.

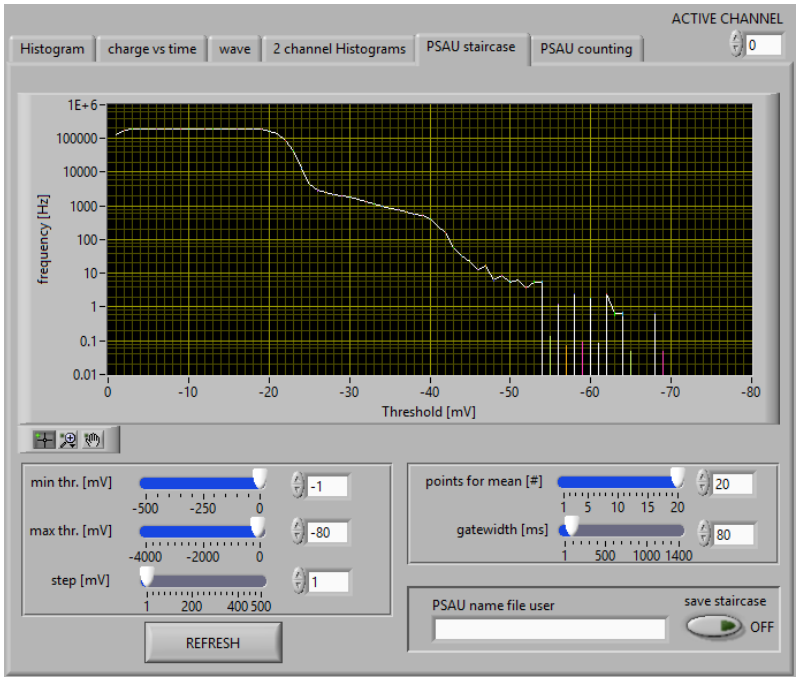

Figure 20: An example of staircase plot of DCR vs trigger threshold voltage

TASKS:
I) Save one such staircase plot and explore for different voltages.
II) Suggest an operating trigger threshold for the voltage used from the obtained plot.

3.4 Measurements with pulsed LED

The LED pulse generator is operated with an attenuator which controls the amplitude of the pulse. Also a high and low frequency switch is present there. Only the internal trigger of the LED driver can be used throughout the experiment. An amplitude of 4.0 can be set to perform the experiment. A charge spectrum can be obtained with this configuration as in figure 17 and all the photo-electron peaks can be fitted with Gaussian functions and the corresponding mean and variance (σ^2) can be calculated. The gain and resolution of the SiPM can be computed from these values. To visualize the resolution of the peaks, the variance of the peaks can be plotted with the peak number and can be found to be like figure 21.

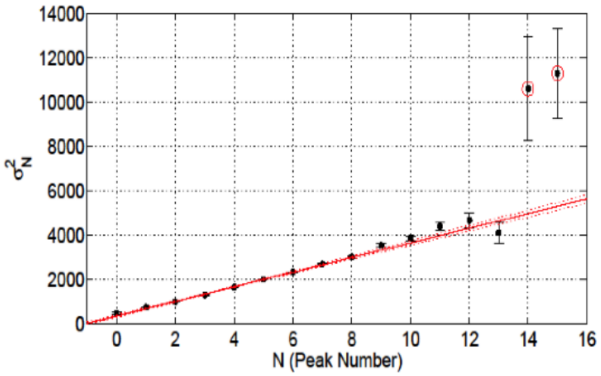

Figure 21: An example plot of peak variance vs the peak number

The **gain, M** of the SiPM is given by,

$$M = \frac{\Delta q_{pp}}{q_e} \tag{2}$$

where, Δq_{pp} is the mean of the charge difference between two consecutive peaks and q_e is the electron's charge in Coulomb. Since we get our charge in terms of ADC channels, this value is needed to be converted to Coulomb charge. Thus, the gain can be expressed as,

$$M = \frac{1}{q_e} \times \frac{\Delta ADCpp}{G_{PSAU}} \times \frac{V_{pp} \times \Delta t}{R_{IN} \times 2^{N_{bit}}} \tag{3}$$

where G_{PSAU} is the PSAU gain applied to the SiPM signal, $V_{pp} = 2V$ is the digitizer dynamic range, R_{IN}=50Ω is the digitizer input impedance, Δt=4ns is the digitizer sampling period and N_{bit}=12 is the digitizer resolution. With these values, M results

$$\boxed{M = \frac{\Delta ADC_{pp}}{G_{PSAU}} \times 2.44 \times 10^5} \tag{4}$$

TASKS:
I) For a fixed voltage, save the charge spectrum (like figure 17) for two different (low and high) intensities of the pulsed LED
II) For a fixed voltage, get a charge spectrum and the corresponding peak variance vs peak number plot (like figure 21)
III) Vary the voltage in small steps and collect the charge spectrum. Calculate ΔADC_{pp}^{avg} with at least three peaks in each voltage, and calculate the corresponding gains. Keep the G_{PSAU} fixed. Draw gain vs bias voltage as in figure 22
IV) Suggest an operating voltage by comparing the plots obtained corresponding to figure 19 and 22

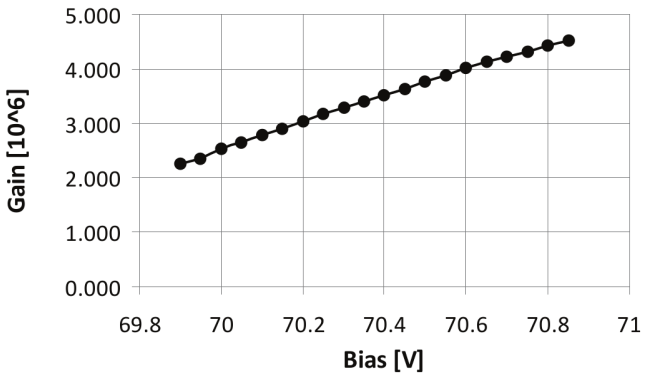

Figure 22: Gain vs bias voltage (right)